



The collision experiment between rolling stones of different shapes and protective cushion in open-pit mines

Chun ZHU, Man-chao HE, Murat KARAKUS, Xiao-hu ZHANG, Zhen GUO

View online: <https://doi.org/10.1007/s11629-020-6380-0>

Articles you may be interested in

[Experimental investigation on debris flow resistance and entrainment characteristics: effects of the erodible bed with discontinuous grading](#)

Journal of Mountain Science. 2022, 19(8): 2397 <https://doi.org/10.1007/s11629-022-7365-y>

[Using computational fluid dynamic simulation with Flow-3D to reveal the origin of the mushroom stone in the Xiqiao Mountain of Guangdong, China](#)

Journal of Mountain Science. 2022, 19(1): 1 <https://doi.org/10.1007/s11629-021-7019-5>

[Effect of freeze-thaw cycles on mechanical behavior of clay-gravel mixtures](#)

Journal of Mountain Science. 2022, 19(12): 3615 <https://doi.org/10.1007/s11629-022-7317-6>

[Mechanical characteristics of soil-rock mixtures containing macropore structure based on 3D modeling technology](#)


Journal of Mountain Science. 2020, 17(9): 2224 <https://doi.org/10.1007/s11629-020-5937-2>



[A calculation model to assess the crack propagation length of rock block in elastic flow](#)


Journal of Mountain Science. 2020, 17(11): 2636 <https://doi.org/10.1007/s11629-020-6207-z>



Original Article


The collision experiment between rolling stones of different shapes and protective cushion in open-pit mines

ZHU Chun^{1,2,3,4}  <https://orcid.org/0000-0003-2867-6478>; e-mail: zhuchuncumb@163.com

HE Man-chao^{3*}  <https://orcid.org/0000-0002-5430-4021>;  e-mail: manchaohecumb@163.com

KARAKUS Murat⁴  <https://orcid.org/0000-0001-6701-1888>; e-mail: murat.karakus@adelaide.edu.au

ZHANG Xiao-hu^{3*}  <https://orcid.org/0000-0001-7216-4758>;  e-mail: zhangxiaohucumb@163.com

GUO Zhen⁵  <https://orcid.org/0000-0003-0485-5586>; e-mail: zhenguo@tongji.edu.cn

*Corresponding author

¹ School of Earth Sciences and Engineering, Hohai University, Nanjing 210098, China

² Engineering Research Center of Development and Management for Low to Ultra-Low Permeability Oil & Gas Reservoirs in West China, Ministry of Education, Xi'an Shiyou University, Xi'an 710021, China

³ State Key Laboratory for Geomechanics & Deep Underground Engineering, Beijing 100083, China

⁴ School of Civil, Environmental and Mining Engineering, The University of Adelaide, Adelaide SA 5005, Australia

⁵ College of Civil Engineering, Tongji University, Shanghai 200092, China

Citation: Zhu C, He MC, Karakus M, et al. (2021) Research on the collision experiment between rolling stones of different shapes and protective cushion in open-pit mines. *Journal of Mountain Science* 18(5). <https://doi.org/10.1007/s11629-020-6380-0>

© Science Press, Institute of Mountain Hazards and Environment, CAS and Springer-Verlag GmbH Germany, part of Springer Nature 2021

Abstract: Though gravel cushions are used worldwide in open-pit mines and railway slopes to control the impact of rolling stones, no universal technical standards have been put in place to guide engineers in their correct design, and few laboratory test results are available with which to characterize collisions between rolling stones and a gravel cushion. We carried out a large number of experiments in which rolling stones made of the same material but differently shaped were dropped from various heights onto cushions with various particle sizes and thicknesses. We investigated the characteristics of the resulting collisions, and the relationships between coefficients of restitution (CORs) of blocks with different shape and release height H , cushion

thickness h and particle diameter d are obtained through linear fitting method. Orthogonal testing reveals the relative influence of block shape, release height, and the particle size and thickness of the cushion on the collision characteristics, which can assist engineers in designing a gravel cushion suitable to the distribution and weathering characteristics of rolling stones in a specific area.

Keywords: Coefficient of restitution (COR); Collision characteristics; Gravel cushion; Rolling stone shape

1 Introduction

Mountainous areas, especially those where geological conditions are complex, are often at high

Received: 01-Aug-2020

Revised: 04-Sep-2020

Accepted: 08-Dec-2020

risk of geological disaster, of which collapse (rolling stone) events are one of the most common. Due to the rainfall, weathering and continuous blasting, rolling stone disasters are more frequent and random in open-pit mines. Rolling stones have a high velocity and numerous modes of movement, including jumping and rolling, they can cause sudden and unpredictable damage to workers and facilities. The term 'rolling stone' broadly refers to blocks separated from the rocky slope by sliding, dumping or falling that begin to jump, roll or slide along steep slopes and finally come to rest on the slope or its foot due to energy loss. The occurrence of rolling stones is mainly influenced by geological factors such as stratigraphic lithology, topographic gradient and geological structure, coupled with precipitation, earthquakes, and human engineering activities. These factors are constantly changing under internal and external dynamic geological forces, and coupling effects give rolling stone disasters a high degree of randomness and unpredictability.

Many scholars have studied the movement characteristics and hazard assessment of rolling stone disasters through field survey, physical model experiment, and numerical simulation (Zhang et al. 2015; Lam et al. 2018; Megan et al. 2018; Meng et al. 2019; Zhu et al. 2019; Zhu et al. 2021a,b; Meng et al. 2020; Tao et al. 2021). Wang et al. (2014) conducted a quantitative evaluation of rockfall risk for Feifeng Mountain in China, the annual probability of occurrence and temporal-spatial probability were calculated. In order to predict the probability of rolling stones attaining a specific range, Frattini et al. (2008) proposed a combined statistical and physical method to evaluate rockfall susceptibility. Andrew et al. (2017) developed a computer model to simulate rolling stone disasters and verified its rationality against a rockfall event in British Columbia. Through a large number of laboratory experiments, Hu et al. (2018) studied the influence of various parameters on the runout range and lateral distribution of a rockfall. The effect of fall height, slope angle and release angle on the COR and loss rate of kinetic energy were further studied by Li et al. (2016) via laboratory experiments. To explain the results of previous tests in Australia that had shown values for the normal COR of greater than one, Buzzi et al. (2012) studied the combined effect of a low impact angle, block angularity, and rotational energy.

Many protection methods against rolling stone

disasters have been developed, and their effectiveness and reasonableness have been validated in a number of studies (Castro et al. 2009; Lambert et al. 2013; Volkwein et al. 2016). Effeindzourou et al. (2017) designed a framework for simulating rockfall protection structures, and applied this framework to explore the dynamic response of a cylindrical module when impacted by a rock. Koo et al. (2017) evaluated the dynamic response of flexible barriers by building a three-dimensional model. Bertolo et al. (2009) conducted tests to assess the overall performance of a draped mesh. Lambert et al. (2018), meanwhile, presented a literature-based criterion that would enable prediction of the performance of embankments in withstanding impacts from rolling stones. The behaviors of IBT-150 and IBT-500 flexible barriers, specifically, were assessed by Castanon-Jano et al. (2018) on the basis of experiments.

The above protective methods have mainly been used to prevent damage from urban areas, railways, and highways. Although they are relatively effective, their construction costs are exorbitant, thus they are not suitable for extensive use to guard against the frequent rolling stone events in open-pit mines. The method universally used to prevent rolling stone disasters in open-pit mines is to lay an energy dissipation cushion (Labiouse et al. 1996; Pichler et al. 2006). Lots of mullock is produced during slope expansion process, and this can be broken into particles of different sizes. These particles are paved on the platform as an energy-consuming layer to reduce the kinetic energy of rolling stones (Zhu et al. 2018). Although the energy dissipation mechanism between cushions and rolling stones of different shapes has been explored a lot (Yuan et al. 2015), few scholars consider the influence of particle size of cushion, especially when the cushion is composed of gravel, and there are no commonly recognized standards for the design of effective gravel cushions. It is thus necessary to conduct experiments to characterize collisions between rolling stones of different shapes and gravel cushions of different particle sizes, and provide engineers with a reference for better rolling stone cushion design.

2 Definition of the Coefficient of Restitution

Several parameters (Table 1) have a significant

Table 1 Parameters influencing rebound trajectory (Labiouse et al. 2009)

Slope features	Block features	Kinematics
Strength	Strength	Translational velocity
Stiffness	Stiffness	Rotational velocity
Roughness	Weigh-size	Collision angle
Inclination	Shape	Configuration of block at impact

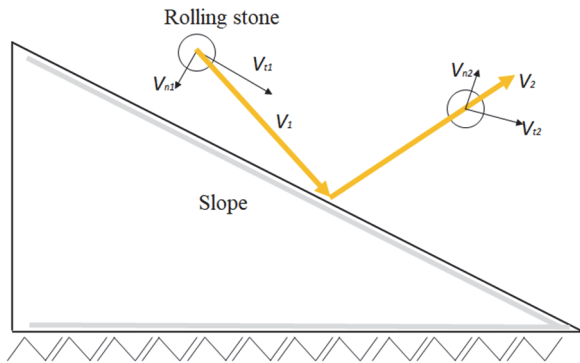


Fig. 1 Collision model between rolling stones and a slope.

influence on rebound, making the prediction of the rebound trajectory difficult. It is generally calculated by way of the coefficient of restitution (COR) (Giani 1992).

When blocks impact a slope (Fig. 1), the COR is normally defined as in Eq. 1 based on the theory of inelastic collision (Chau et al. 2002):

$$V_{COR} = \frac{V_2}{V_1} \tag{1}$$

where V_1 and V_2 are the velocities of the block before and after impacting the slope, respectively (m/s).

The kinetic COR comprises normal and tangential components in respect to the slope surface. The normal (R_n) and the tangential (R_t) coefficients of restitution are defined as Eq.2:

$$R_n = \frac{V_{n2}}{V_{n1}} \quad R_t = \frac{V_{t2}}{V_{t1}} \tag{2}$$

where V_{n1} and V_{n2} are the normal components and V_{t1} and V_{t2} are the tangential components of velocity before and after the collision, respectively (m/s).

The kinetic energy coefficient of restitution R_E is defined by the ratio of kinetic energies before and after impact, which is shown as Eq.3:

$$R_E = \frac{E_2}{E_1} \tag{3}$$

where E_1 and E_2 are the kinetic energy before and after the impact, respectively.

The kinetic energy of the block is the sum of its translational (E_t) and rotational (E_r) energies, as

shown in Eq.4:

$$E = E_t + E_r = 0.5mv^2 + 0.5I\omega^2 \tag{4}$$

where m is the mass of the block, I is its moment of inertia, and ω is its angular velocity.

Thus the kinetic energy coefficient of restitution R_E can be also represented as Eq.5:

$$R_E = \frac{(E_{t2} + E_{r2})}{(E_{t1} + E_{r1})} = \frac{0.5mv_2^2 + 0.5I\omega_2^2}{0.5mv_1^2 + 0.5I\omega_1^2} \tag{5}$$

where E_{t1} and E_{t2} are the translational energy before and after the impact. E_{r1} and E_{r2} represent the rotational energy before and after the impact. ω_1 and ω_2 denote the angular velocity before and after the impact, respectively.

3 Experimental Studies

3.1 Materials and equipment preparation

To explore the collision characteristics between rolling stones of different shapes and gravel cushions conveniently, because of the properties of quick setting and strengthening of gypsum material, blocks of different shapes were formed out of gypsum and water to simulate rolling stones (Li et al. 2016). A moisture content of 40% was used for all of the blocks in this study following Chau et al.'s (2002) adoption of a block moisture content of 30%-50% in indoor rolling stone tests.

A previous study showed that rolling stones of different shapes impacting a plate gave very different results (Asteriou et al. 2016), so various cushion designs were used in this study for each block shape. The effects of block shape on the collision characteristics are studied here through the use of blocks of the same weight but of different shapes: 3 cm-radius spherical blocks, 4.84 cm cubic blocks, 7.68 cm × 3.84 cm × 3.84 cm cuboid blocks, and 4.16 cm-diameter, 8.32 cm-high cylindrical blocks (Fig. 2), the volume of all the blocks are about 113 cm³.

The uniaxial compressive strength of the gypsum blocks was evaluated by breaking standard cylindrical samples 5 cm in diameter and 10 cm in height under uniaxial compression. 12 compression tests were carried out to reduce the error in the experiment and yielded an average value of compressive strength of 6.36 MPa, in addition, the cushion is paved on the base and has a good buffering effect. This indicates that the gypsum blocks cannot be destroyed during their period of motion (Li et al. 2016; Wang et al.



Fig. 2 Gypsum blocks of different shapes made from the same material.

2021a, b).

In the open-pit mines, lots of mullock is produced during slope expansion process, and this can be broken into particles of different sizes. The particles are paved on the platform as an energy-consuming layer. Therefore, the gravel cushion and rolling stones are basically the same material in the open-pit mines. To simulate cushions composed of different particle sizes, many gypsum boards were broken into granular groups of different sizes (Fig. 3), and the fragments were passed through sieves of different calibers to divide them into 2 mm particle group, 6 mm particle group, 10 mm particle group, 14 mm particle group, 18 mm particle group and 24 mm particle group. Because the difference of particle diameter size between each group is too small, the effect of particle size gradation between each group can be basically ignored.

A gypsum base measuring 40 cm long, 40 cm wide and 6 cm high was built to simulate the platform of an open-pit mine, and gypsum particles are laid on the base. To reduce interference with block velocity measurements, the gypsum cushion was blackened. To simulate cushions of different thickness conveniently, 40 cm-long × 40 cm-wide × 2 cm-high hollow gypsum boards with were made and a 30 cm-long × 30 cm-wide × 2 cm-high section was cut out of the center of each board. The hollow gypsum boards can be stacked according to the requirements for cushion thickness; the hollow parts of the stacked boards are then filled with gypsum particles, keeping them in a dense state that simulates gravel cushions in field engineering applications (Fig. 4).

The rolling stone launcher is composed of a movement tube, telescoping shoring column, dial, and fixed base (Fig. 5). Two digital cameras (1024×1024 pixels) were placed symmetrically 0.9 m away from the cushion. The location and characteristics of blocks can be measured by the two cameras at a time interval of 1/200 s.

3.2 Experimental program

To study the effects of rolling stone shape on the characteristics of their collisions with cushions of different thicknesses and particle sizes, blocks of the four shapes (cylinder, sphere, cuboid, and cube) were released from 0.5 m, 1.0 m, 1.5 m and 2.0 m to impact the cushion. As the release height H increased, the

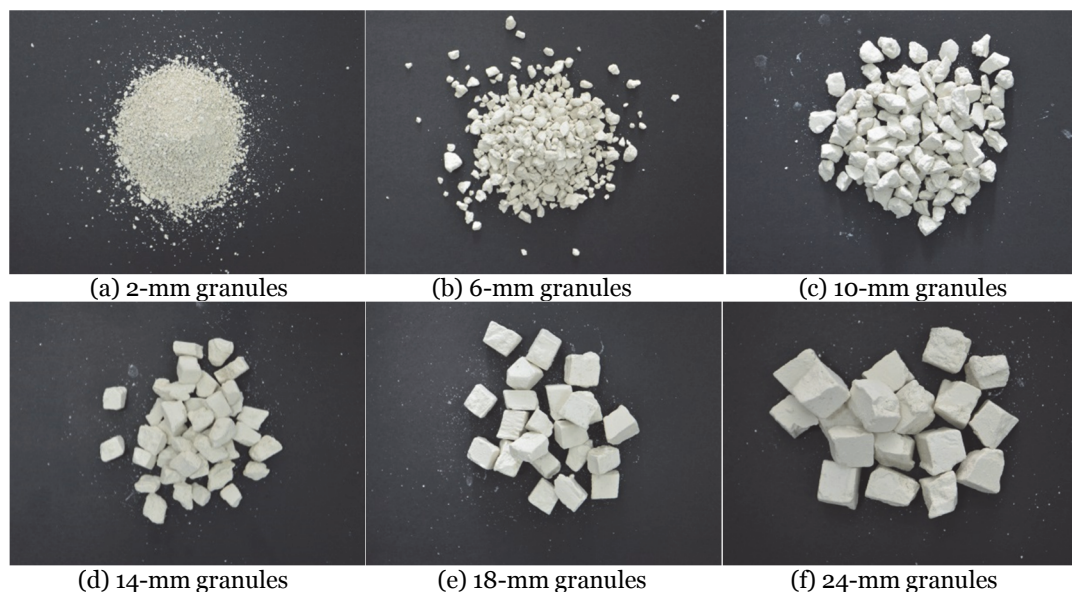


Fig. 3 Groups of different gypsum diameter sizes.

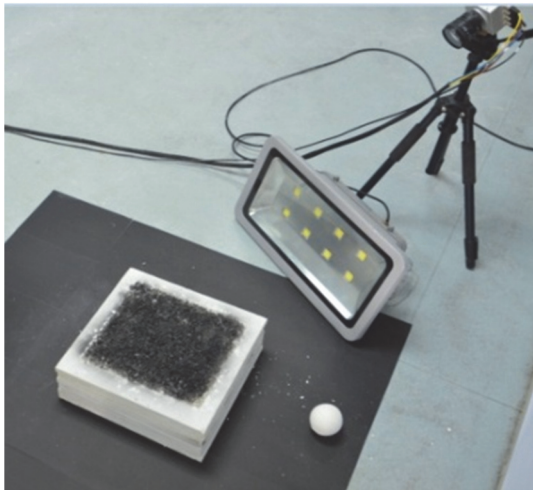


Fig. 4 Simulation of a gravel cushion (Zhu et al. 2018).

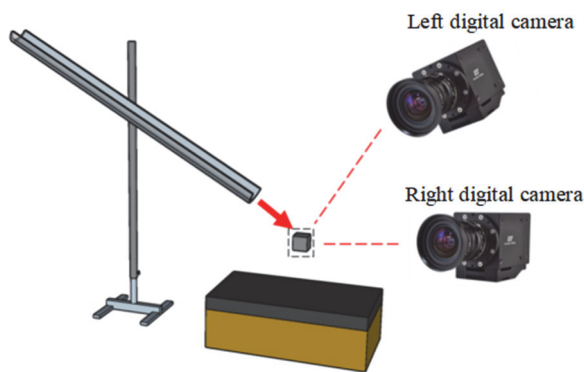


Fig. 5 Rolling stone launcher device.



Fig. 6 Cushion after a block impact experiment.

length of the blocks of rolling stones motion in the tube also increased. The tube was made of steel and the inside of the pipe is smooth, thus the friction between specimens and tube was small, and the loss of kinetic energy of specimen due to friction in the

tube was relatively small. For the cylindrical and cuboid blocks, the length side of blocks towards to the moving direction, so that the blocks can roll along the launch tube. Cushions 4 cm, 8 cm and 12 cm thick were formed from particles of different sizes from 2 mm to 24 mm, respectively. After the hollow parts of the stacked boards were filled with gypsum particles, a wood plate was placed on top of the gypsum particles, and then a 20 kg weight was placed on the wood plate to compact the gravel cushion for 5 minutes. If the gravel cushion is sunken or still protruding, the gypsum will be added or removed until the gravel cushion is flat. The COR values from the experiment were calculated on the basis of the ratio of block velocities before and after the collision, as described in Eq.1. The experiment is carried out by setting the release angle of the block and releasing it, whereupon it rolls through the tube to impact the gravel cushion surface. Fig. 6 shows a cushion after the collision of a block.

Because the contact surfaces between the blocks and particles differ greatly, there is high uncertainty in collision characteristics, especially for the cuboid and cylindrical blocks. An increase in particle size will also affect the uncertainty. Therefore, the “three in five tests for the mean” method was adopted in this research, i.e., each test was repeated five times, and the middle three values were adopted to calculate the mean; the mean is considered the test result. During the experimental process, the location of the block is automatically captured by the two cameras, and its velocity and kinetic energy can be calculated on the basis of change in location with time, as shown in Fig. 7.

3.3 Experimental results

To constrain the controlling effects of paving the platform with a cushion, rolling stones of the four shapes were first released from different heights to impact the uncushioned base. The CORs were calculated and are plotted in Fig. 8.

The base was then paved with cushions of particles with different diameters d (2 mm, 6 mm, 10mm, 14 mm, 18 mm and 24 mm) and thicknesses h (4cm, 8cm and 12 cm), and subjected to further impact experiments. The CORs calculated for the resulting collisions between blocks and cushions are plotted in Figs. 9–12.

According to the calculation results of CORs between the cylindrical blocks and different cushion

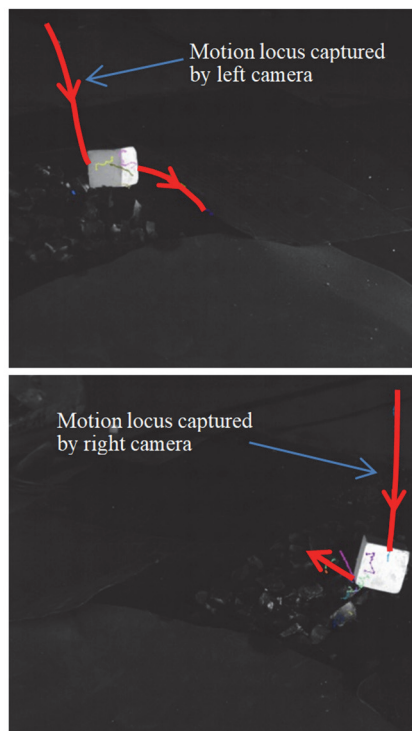


Fig. 7 Location and motion characteristics of blocks are captured automatically by camera

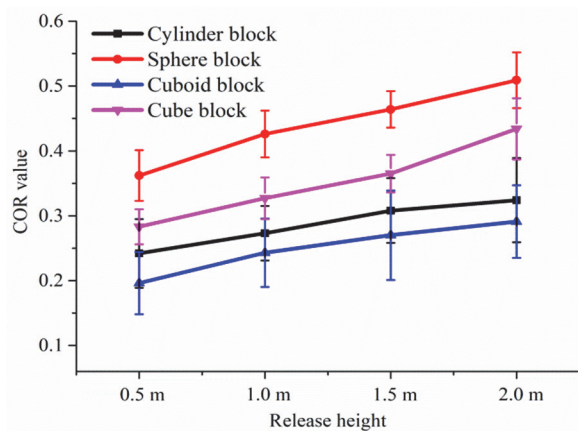


Fig. 8 Coefficients of restitution (CORs) (Mean ± SD) of blocks colliding with the uncushioned base. (Error bars: one standard deviation)

(Fig. 10), the relationship between CORs of cylindrical blocks and release height H , cushion thickness h and particles d can be obtained through linear fitting method, and the formula is shown as Eq.6:

$$\text{COR} = 0.0181889H - 0.215625h + 1.95696d \quad (6)$$

$$R^2 = 0.921237$$

where R^2 is the coefficient of determination.

According to the calculation results of CORs between the spherical blocks and different cushion (Fig. 10), the relationship between CORs of spherical

blocks and release height H , cushion thickness h and particle diameter d can be obtained through linear fitting method, and the formula is shown as Eq.7:

$$\text{COR} = 0.0321333H - 0.271875h + 2.41821d \quad (7)$$

$$R^2 = 0.961107$$

According to the calculation results of CORs between the cuboid blocks and different cushion (Fig. 11), the relationship between CORs of cuboid blocks and release height H , cushion thickness h and particles d can be obtained through linear fitting method, and the formula is shown as Eq.8:

$$\text{COR} = 0.0219667H - 0.231771h + 2.61864d \quad (8)$$

$$R^2 = 0.962163$$

According to the calculation results of CORs between the cubic blocks and different cushion (Fig. 12), the relationship between CORs of cubic blocks and release height H , cushion thickness h and particles d can be obtained through linear fitting method, and the formula is shown as Eq.9:

$$\text{COR} = 0.0242556H - 0.257813h + 2.29064d \quad (9)$$

$$R^2 = 0.957114$$

3.4 Discussion of experimental results

As can be seen from the above figures, extremely variable COR values arose when rolling stones of different shapes but the same material properties and kinetic energy collided with the same gravel cushion. Overall, the collision of a spherical rolling stone with a cushion gives the largest COR, followed, from largest to smallest, by that of a cube, a cylinder, and a cuboid. Because cylindrical and cuboid rolling stones have different contours rotationally, these rolling stones are more sensitive to the particle size of the cushion. When the particle size is large, the contact interface between the particles and the rolling stones can differ widely, and the range of COR values of the collision is also wide, so the deviations of the COR results are relatively large.

When rolling stones are released to collide with the uncushioned base, the COR of the collision is relatively large. As the thickness of the cushion is increased, there is a marked decrease in the COR, especially for cuboid rolling stones. Because the collision between a rolling stone and the cushion occurs as an ephemeral process and involves an intricate deformational process, the controlling effects of cushions with different thicknesses and particle sizes are extremely variable. As the release height is

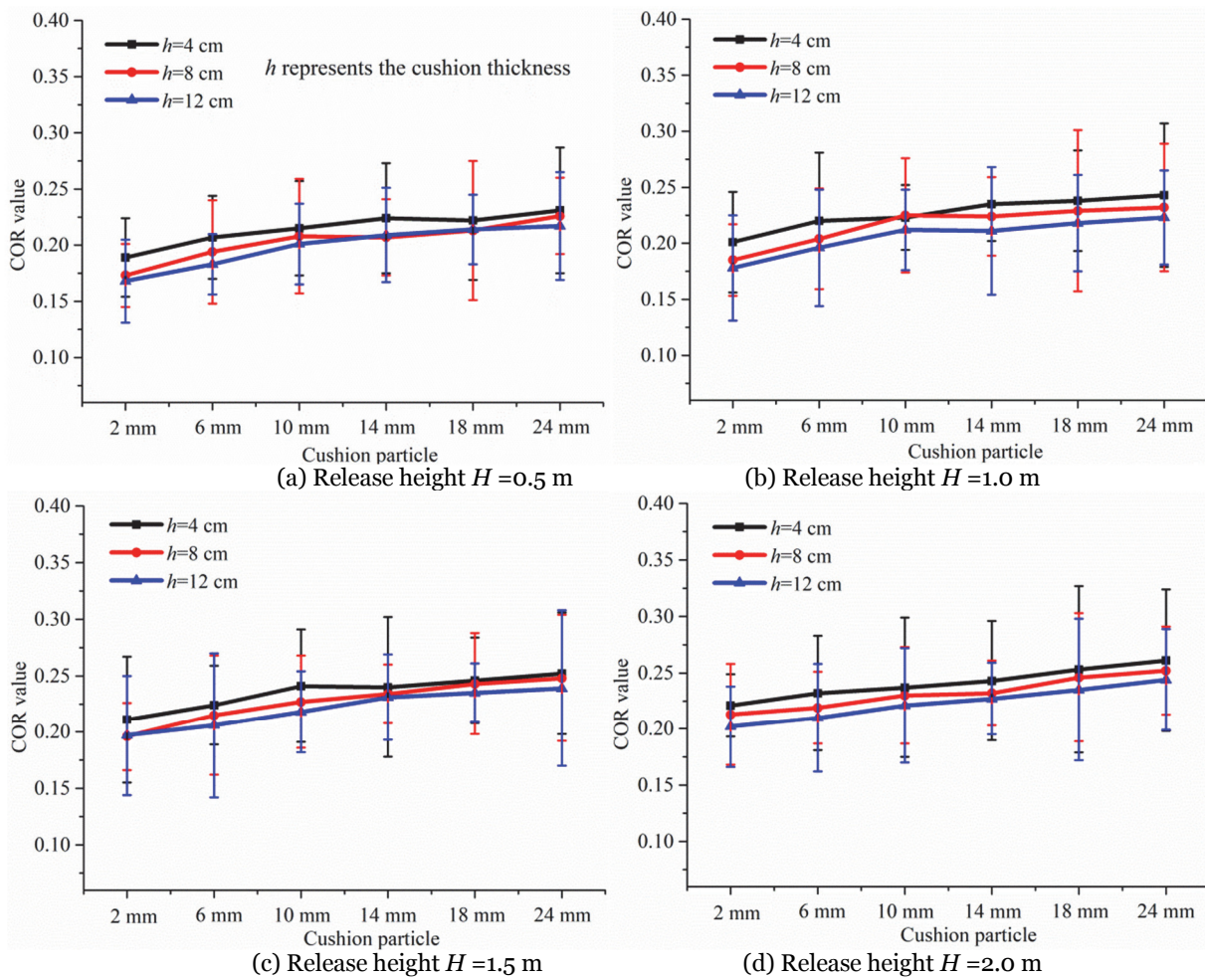


Fig. 9 Coefficients of restitution (CORs) of collision between cylindrical blocks released from different heights and cushions.

increased, the COR of collision between rolling stones and the cushion also grows. The influence of rolling stone shape on the COR is more significant when rolling stones are released from a small height than from a greater height, and cuboids are the most sensitive to this influence, followed by cylinders.

However, the rate of decrease in the COR value with increasing cushion thickness reduces as thickness becomes greater, and the range in the decrease rate of rolling stones with a high energy is smaller than that of rolling stones with a low energy. As the particle size of the cushion is decreased, the COR of collision decreases rapidly, but small particles more strongly reduce the COR of collision when blocks with a low kinetic energy collide with the cushion than blocks with a high kinetic energy. That is, when potential rolling stones are located at a relatively high position, the thickness and particle size of the cushion should both be considered, while if they are located at a relatively low position, a

relatively small particle size is the most important factor in the design of the gravel cushion.

4 Effect of Each Factor on COR

Orthogonal tests were designed to investigate the degree of influence of the four factors studied, i.e., block shape, release height, and cushion particle size and thickness, on the characteristics of collision between a block and a cushion and to identify the main influencing factor (Zhu et al. 2018). The COR of collision between blocks and cushions and the damage depth, L , of the cushion are taken as the test indices for evaluating the controlling effect of the cushion on rolling stones (Pichler et al. 2005). The damage depth (L) represents the depth of the cushion that is influence by block-collision with the cushion and quantifies the degree of damage to the cushion. The four factors and their four values are shown in

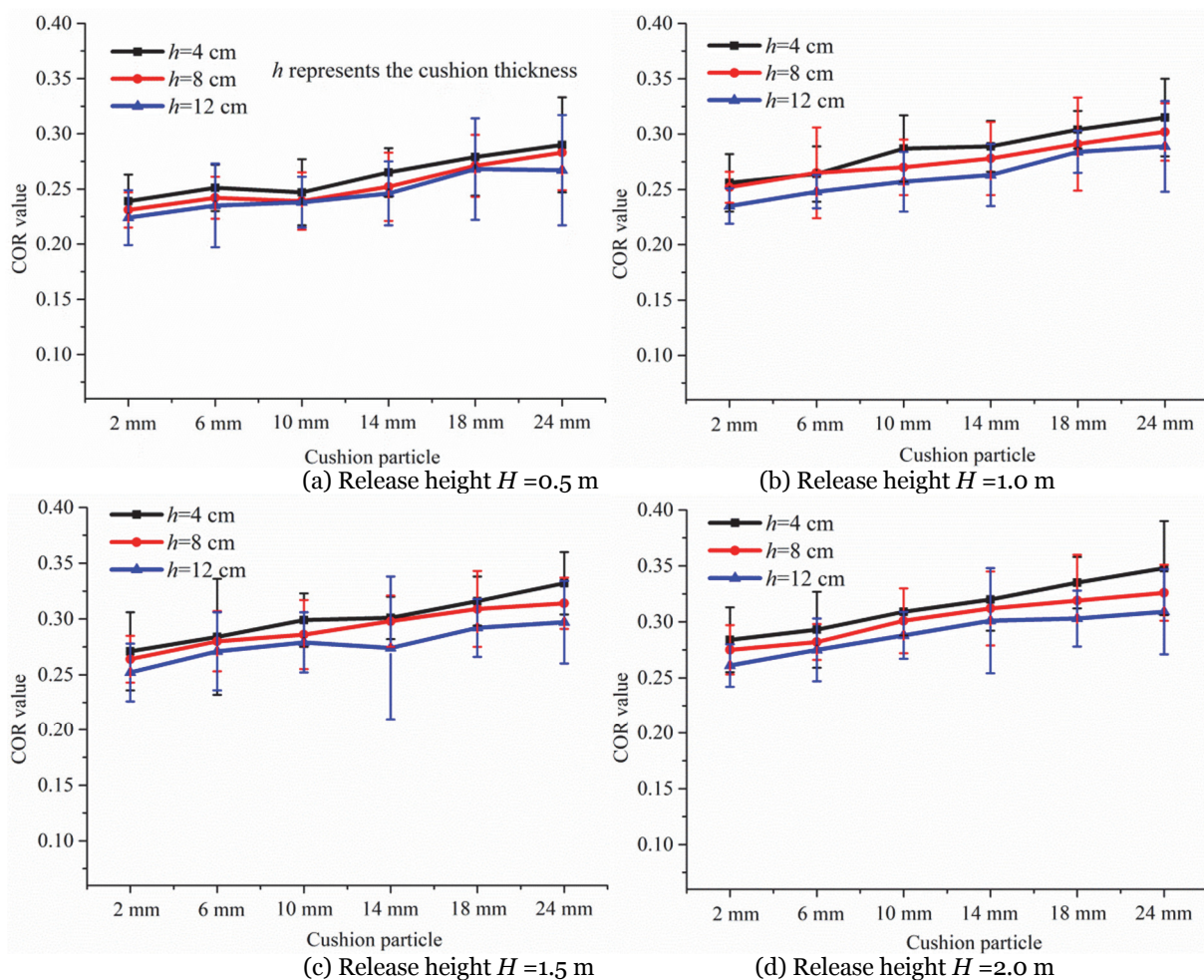


Fig. 10 Coefficients of restitution (CORs) of collision between spherical blocks released from different heights and cushions

Table 2 Values of selected parameters for COR evaluation

Factor values	Rolling stone shape	Cushion thickness h (cm)	Release height H (m)	Particle diameter d (mm)
Value 1	Cylinder	4	0.5	2
Value 2	Sphere	6	1.0	6
Value 3	Cuboid	8	1.5	10
Value 4	Cube	10	2.0	14

Table 2.

In order to ensure the accuracy of the tests, the $L_{16} (4^5)$ test design was adopted, and each test adopted the “three in five tests for the mean” method. The experimental results are shown in Table 3.

where $L_{16} (4^5)$ represents 16 designed tests are carried out, this test design can be applied to less than 5 parameters with 4 values.

Range analysis is adopted to analyze the results of the orthogonal test. The parameters, including block shape, particle size d , cushion thickness h , and release height H , are the influencing factors and are set as (X_1, X_2, X_3, X_4) , each factor has four levels. P_{xy} is the test result for level y of factor X , K_{xy} values are

obtained by summing all the P_{xy} results, and dividing K_{xy} by the level number N_y gives the mean k_{xy} , as is shown in Eq.10, which is used to estimate the best value and combination for each factor. R_y is the difference between the maximum and minimum value of k_{xy} in a column and reflects the degree of influence of the factor on the test index (Zhu et al. 2018). A large R_y value represents a high degree of influence, so this can be used to rank the degree of influence of the different factors.

$$k_{xy} = \frac{K_{xy}}{N_y} = \frac{\sum P_{xy}}{N_y} \tag{10}$$

where K_{xy} is the statistical parameter of factor x at level y .

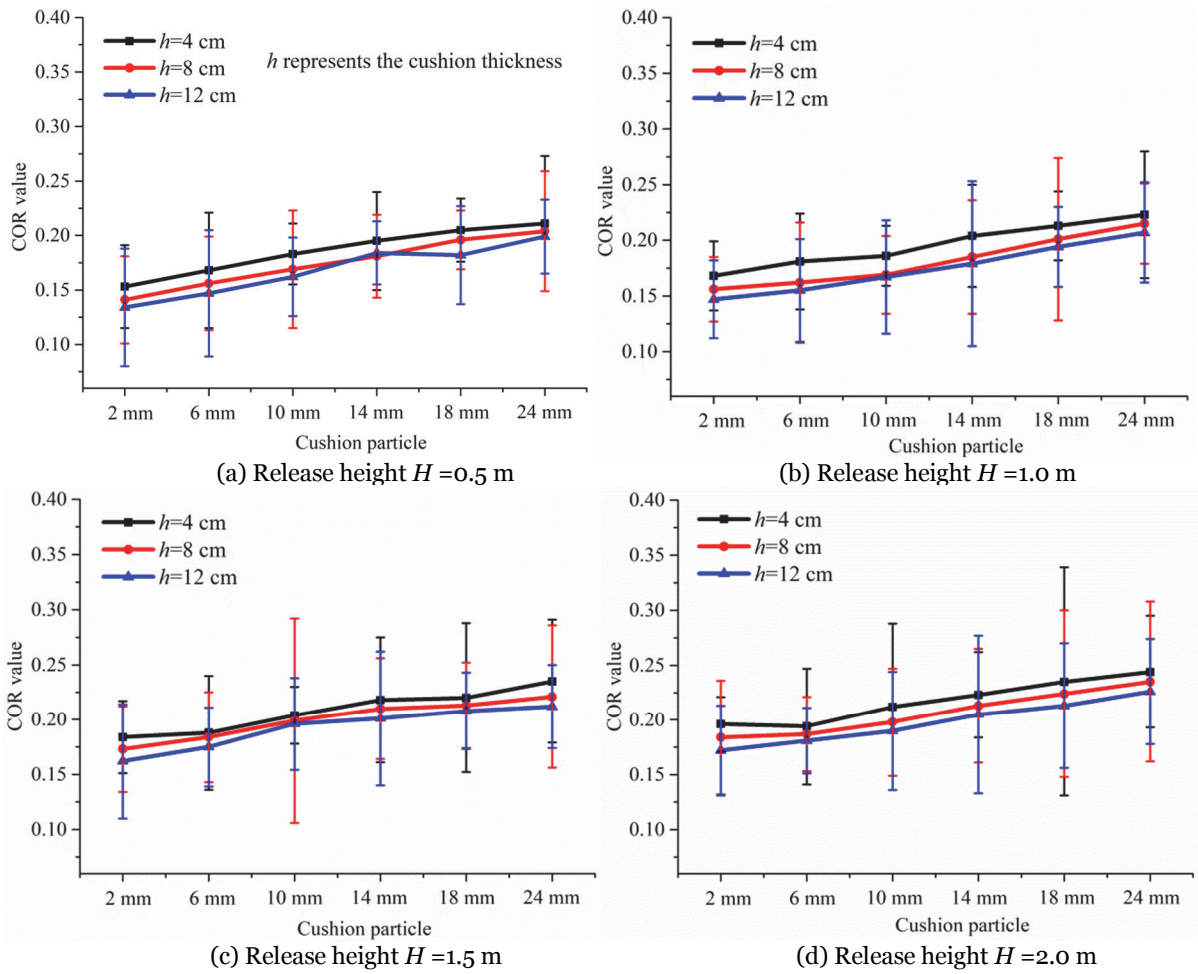


Fig. 11 Coefficients of restitution (CORs) of collision between cuboid blocks released from different heights and cushions.

Table 3 Experimental results of orthogonal testing

Test number	Rolling stone shape	Cushion thickness (h , cm)	Release height (H , m)	Particle diameter (d , mm)	COR of collision between rolling stones and cushion (Mean/Std dev)	Damage depth of cushion (L , cm) (Mean/std dev)
1	Cylinder	4	0.5	2	0.194/0.043	0.92/0.105
2	Cylinder	6	1.0	6	0.213/0.035	1.35/0.168
3	Cylinder	8	1.5	10	0.228/0.049	1.47/0.093
4	Cylinder	10	2.0	14	0.226/0.027	1.64/0.129
5	Sphere	4	1.0	10	0.285/0.032	1.11/0.043
6	Sphere	6	0.5	14	0.252/0.021	0.52/0.031
7	Sphere	8	2.0	2	0.281/0.034	3.03/0.091
8	Sphere	10	1.5	6	0.288/0.028	2.40/0.084
9	Cuboid	4	1.5	14	0.224/0.051	1.01/0.106
10	Cuboid	6	2.0	10	0.207/0.043	1.53/0.073
11	Cuboid	8	0.5	6	0.159/0.054	0.68/0.057
12	Cuboid	10	1.0	2	0.145/0.046	1.69/0.083
13	Cube	4	2.0	6	0.263/0.028	2.26/0.056
14	Cube	6	1.5	2	0.231/0.026	2.58/0.039
15	Cube	8	1.0	14	0.242/0.047	0.75/0.065
16	Cube	10	0.5	10	0.210/0.032	0.63/0.041

The COR of the rolling stone–cushion collision and the damage depth, L , of the cushion are taken as the influenced indices in the range analysis. The

analysis results are shown in Table 4.

A tendency figure can be used to reflect the effects of each factor on the influenced indices and

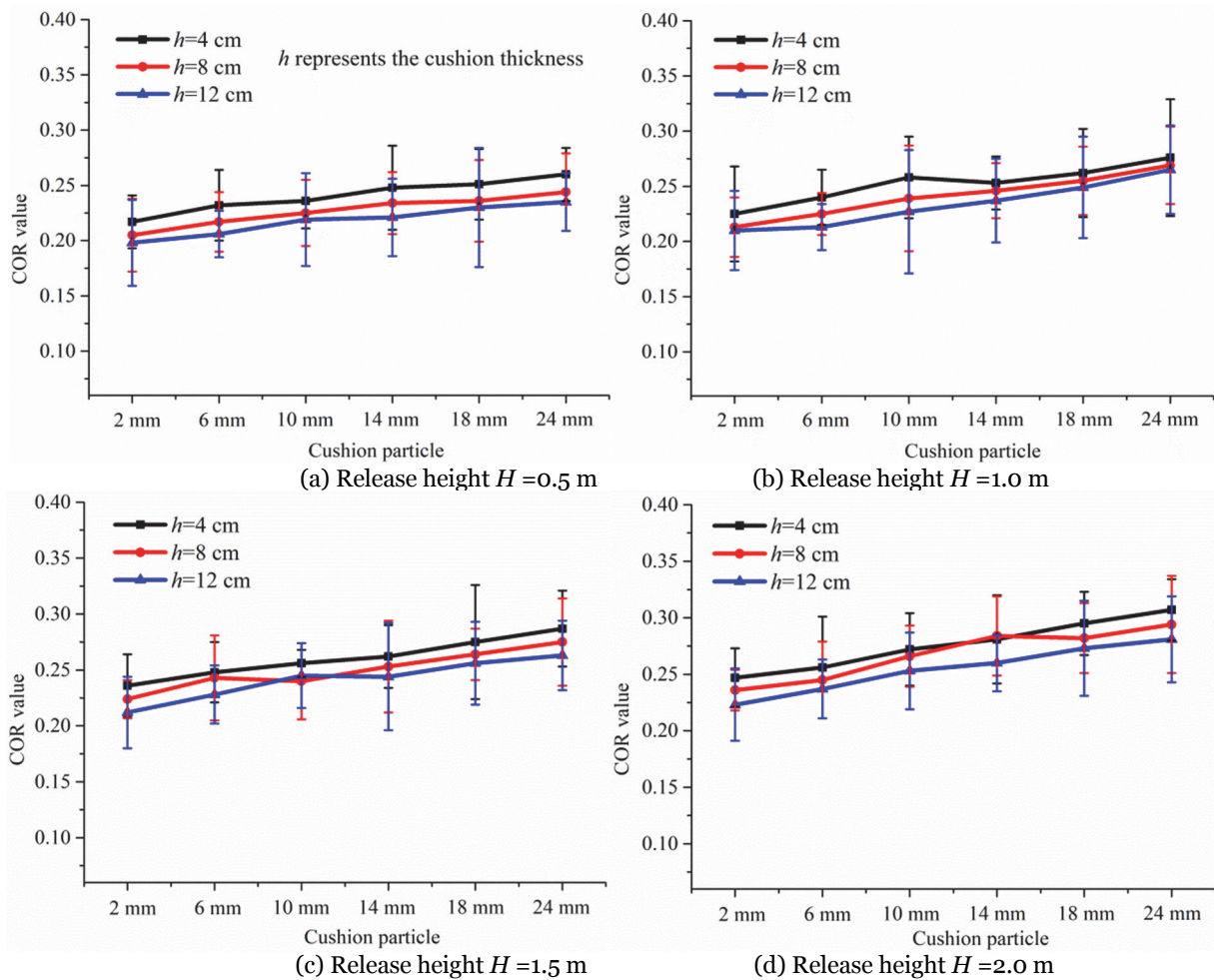


Fig. 12 Coefficients of restitution (CORs) of collision between cubic blocks released from different heights and cushions.

Table 4 Range analysis for orthogonal experimental results

Influenced indices	Values	Rolling stone shape	Cushion thickness (h , cm)	Released height (H , m)	Particle diameter (d , mm)
COR of collision between rolling stones and cushions	k_{x1}	0.215	0.242	0.204	0.213
	k_{x2}	0.277	0.226	0.221	0.231
	k_{x3}	0.184	0.228	0.243	0.233
	k_{x4}	0.237	0.217	0.244	0.236
	R_y	0.093	0.025	0.040	0.023
Damage depth of cushion L	k_{x1}	1.35	1.33	0.69	2.06
	k_{x2}	1.77	1.50	1.23	1.67
	k_{x3}	1.23	1.48	1.87	1.19
	k_{x4}	1.56	1.59	2.12	0.98
	R_y	0.54	0.26	1.43	1.08

enable the best combination of factors to be identified. The tendency figures are shown in Figs. 13 and 14.

In the current experimental condition, the degrees of influence of the four factors on the COR of collision are ranked: rolling stone shape > release height (H) > cushion thickness (h) > particle size (d). The best combination of parameters is A3B2C1D1; i.e.,

when the rolling stone is a cuboid, $h=6$ cm, $H=0.5$ m, and $d=2$ mm the COR value of the collision is smallest (Fig. 13).

In the current experimental condition, the degrees of influence of the four factors on the damage depth, L , of the cushion are ranked: release height (H) > particle size (d) > rolling stone shape > cushion

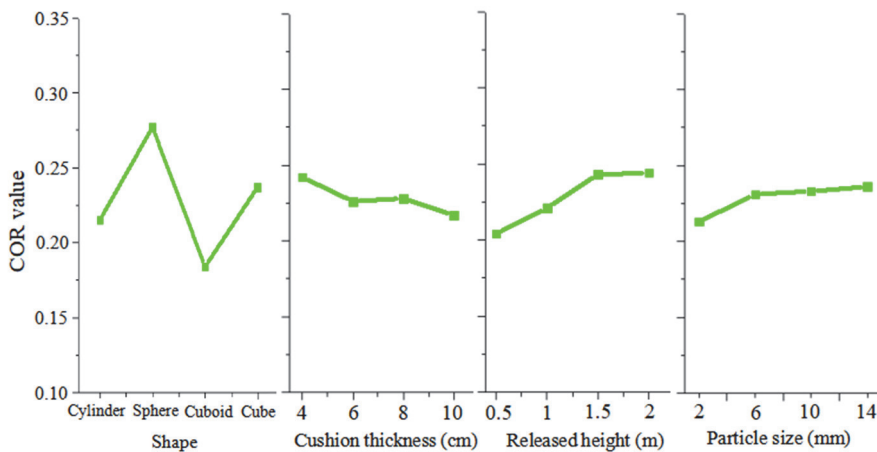


Fig. 13 Tendencies of the influence of each factor on the COR of the collision.

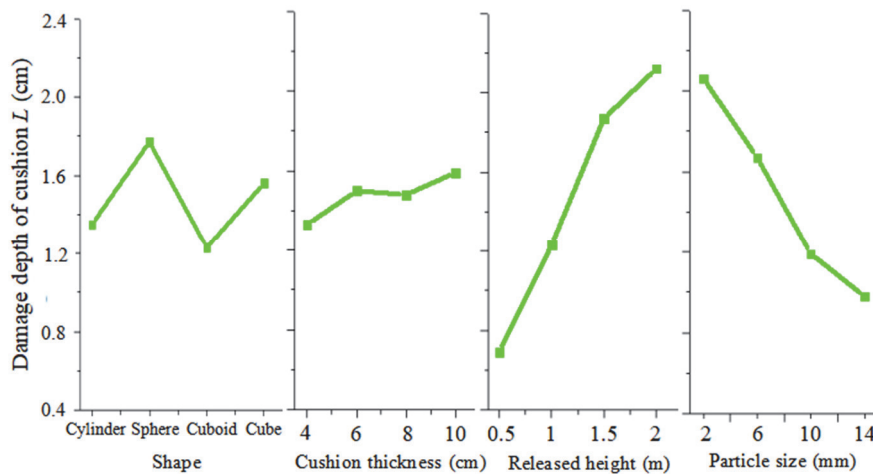


Fig. 14 Tendencies of the influence of each factor on the damage depth L of the cushion.

thickness (h). The best combination of parameters is A1B1C1D4; i.e., when the rolling stone is a cuboid, $h=4$ cm, $H=0.5$ m, and $d=14$ mm, the damage depth, L , of the cushion is the shallowest (Fig. 14).

The shape of rolling stones has the greatest effect on the COR of the collision, followed, in decreasing order, by the release height of the stones, the cushion thickness, and the cushion particle size. Fig. 13 shows that cuboid blocks have the lowest COR during the impact process, while spherical blocks have the largest COR values. This is because the surface of a sphere is smoother and rounder than that of the other shape, and it will suffer less resistance than during the rolling process, causing it to have relatively high kinetic energy. Additionally, the area over which it contacts the cushion is relatively small, the pressure applied per unit area on the cushion is high, and thus the cushion absorbs relatively less of the energy of a spherical block than of blocks of other shapes, causing

the damage depth to be deeper than for blocks of other shapes.

The height from which rolling stones are released has the greatest effect on the damage depth, L , of the cushion, followed by particle size (Fig. 14). This is because a block with relatively high kinetic energy is more destructive to the cushion, and when the particle size is small, the particles are easily pressed into gaps between other particles under the impact. The cushion thickness and block shape have a much lower degree of influence than the other factors. On the whole, the controlling effects of a cushion on rolling stones are better where the cushion particle size is smaller and its thickness is larger, but such cushions are also easier to damage, leading to an increase in the frequency with which the gravel cushion must be repaired.

Thus the distribution and weathering characteristics of rolling stones should be considered comprehensively when designing the cushion so that it can have the greatest possible effectiveness and durability.

5 Conclusion

Collision experiments between rolling stones and gravel cushions were carried out, and the influences of the shape of the rolling stones, their release height, and cushion thickness and particle size on the characteristics of the collision were studied. Four conclusions have been reached.

1. Through a large number of laboratory tests, it was found that the CORs of collisions between rolling stones of different shapes and the same cushion vary widely. The COR of spherical blocks is the largest,

followed, in order of decreasing magnitude, by cubic blocks, cylindrical blocks, and cuboid blocks. The deviations in the COR are relatively high for cuboid and cylindrical blocks. The relationships between CORs of blocks with different shape and release height H , cushion thickness h and particles d are obtained through linear fitting method.

2. Experimental collisions of blocks with cushions of different thicknesses and particle sizes showed that the COR of collision decreases with an increase in cushion thickness, but the decrease rate of the COR becomes smaller at greater cushion thicknesses, and the range in the decrease rate of rolling stones with a high energy is smaller than in rolling stones with a low energy. As cushion particle size is decreased, the COR of collision also decreases, but the range in the decrease rate of rolling stones with a low kinetic energy is larger than in those with a high kinetic energy. Thus, the position of potential rolling stones can be used to understand whether the thickness or particle size of the cushion is more important to the cushion design.

3. According to the results of orthogonal testing, in the current experimental condition, the shape of rolling stones has the greatest effect of the factors considered on the COR of collision; cuboid blocks have the lowest COR during impact, and spherical blocks have the largest COR value. The degree of influence of the other factors on the COR of collision can be ranked, from greatest to least, as the release height of the rolling stones, cushion thickness, and cushion particle size. Furthermore, the release height of rolling stones and the cushion particle size have significant effects on the damage depth, L , of the cushion. A block with relatively high kinetic energy is more destructive to the cushion than those with lower

kinetic energy, and particles are more easily pressed into gaps between other particles under impact when the particle size is small. Block shape and cushion thickness have a far weaker effect on the damage depth than the other factors.

4. Overall, thick cushions with a small particle size have better controlling effects on rolling stones, but such cushions are easier to be destroyed by rainfall, wind and collision, leading to an increased repair frequency. Thus, the thickness and particle size of the cushion should be considered comprehensively in the design of a cushion according to the shape, distribution and weathering characteristics of potential rolling stones. In the actual engineering, the construction cost, durability capability, and prevention effect of the cushion also should be taken into account comprehensively. This finding can guide the design of gravel cushion for mitigating hazard from rolling stones in the open-pit mines to some extent.

Acknowledgments

This work was supported by the Fundamental Research Funds for the Central Universities (No. B210201001), the open fund of Key Laboratory of Rock Mechanics and Geohazards of Zhejiang Province (No. ZJRMG-2020-02), the open fund of Engineering Research Center of Development and Management for Low to Ultra-Low Permeability Oil & Gas Reservoirs in West China, Ministry of Education (No. KFJJ-XB-2020-7), and the Research and Development Project of Guizhou University of Engineering Science (No. G2018016).

References

- Asteriou P, Tsiambaos G (2016) Empirical model for predicting rockfall trajectory direction. *Rock Mech Rock Eng* 49:927-941.
<https://doi.org/10.1007/s00603-015-0798-7>
- Andrew M, Oldrich H (2017) Theory and calibration of the Pierre 2 stochastic rock fall dynamics simulation program. *Can Geotech J* 54(1): 18–30.
<https://doi.org/10.1139/cgj-2016-0039>
- Buzzi O, Giacomini A, Spadari M (2012) Laboratory investigation on high values of restitution coefficients. *Rock Mech Rock Eng* 45: 35-43.
<https://doi.org/10.1007/s00603-011-0183-0>
- Bertolo P, Oggeri C, Peila D (2009) Full-scale testing of draped nets for rock fall protection. *Can Geotech J* 46(3): 306-317.
<https://doi.org/10.1139/T08-126>
- Chau KT, Wong RHC, Wu JJ (2002) Coefficient of restitution and rotational motions of rockfall impacts. *Int J Rock Mech Min Sci* 39(1): 69-77.
[https://doi.org/10.1016/S1365-1609\(02\)00016-3](https://doi.org/10.1016/S1365-1609(02)00016-3)
- Castro-Fresno D, López QL, Blanco-Fernandez E (2009) Design and evaluation of two laboratory tests for the nets of a flexible anchored slope stabilization system. *Geotech Test J Journal* 32(4):315-324.
<https://doi.org/10.1520/GTJ101218>
- Castanon-Jano L, Blanco-Fernandez E, Castro-Fresno D, et al. (2018) Use of explicit FEM models for the structural and parametrical analysis of rockfall protection barriers. *Eng Struct* 166: 212-216.
<https://doi.org/10.1016/j.engstruct.2018.03.064>
- Effeindzourou A, Thoeni K, Giacomini A (2017) Efficient

- discrete modelling of composite structures for rockfall protection. *Comput Geotech* 87: 99-114.
<https://doi.org/10.1016/j.compgeo.2017.02.005>
- Frattini P, Crosta GB, Carrara A, et al. (2008) Assessment of rockfall susceptibility by integrating statistical and physically-based approaches. *Geomorphology* 94(3-4): 419-437.
<https://doi.org/10.1016/j.geomorph.2006.10.037>
- Giani GP (1992) Rock slope stability analysis. Balkema, Rotterdam. <https://doi.org/10.1139/t94-039>
- Hu J, Li SC, Shi SS (2018) Experimental study on parameters affecting the runout range of rockfall. *Adv Civil Eng* 2018(1): 1-9.
<https://doi.org/10.1155/2018/4739092>
- Koo RCH, Kwan JSH, Lam C, et al. (2017) Dynamic response of flexible rockfall barriers under different loading geometries. *Landslides* 14(3): 905-916.
<https://doi.org/10.1007/s10346-016-0772-9>
- Lambert S, Kister B (2018) Efficiency assessment of existing rockfall protection embankments based on an impact strength criterion. *Eng Geol* 243: 1-9.
<https://doi.org/10.1016/j.enggeo.2018.06.008>
- Lam C, Yong ACY, Kwan JSH (2018) Overturning stability of L-shaped rigid barriers subjected to rockfall impacts. *Landslides* 15(7): 1347-1357.
<https://doi.org/10.1007/s10346-018-0957-5>
- Li LP, Sun SQ, Li SC (2016) Coefficient of restitution and kinetic energy loss of rockfall impacts. *KSCE J Civil Eng* 20(6): 2297-2307.
<https://doi.org/10.1007/s12205-015-0221-7>
- Lambert S, Bourrier F (2013) Design of rockfall protection embankments: A review. *Eng Geol* 154: 77-88.
<https://doi.org/10.1016/j.enggeo.2012.12.012>
- Labieuse V, Descocedres F, Montani S (1996) Experimental study of rock sheds impacted by rock blocks. *Struct Eng Int* 6(3):171-176.
<https://doi.org/10.2749/101686696780495536>
- Labieuse V, Heidenreich B (2009) Half-scale experimental study of rockfall impacts on sandy slopes. *Nat Hazards Earth Syst Sci* 9(6):1981-1993.
<https://doi.org/10.5194/nhess-9-1981-2009>
- Megan VV, Hutchinson DJ, Bonneau DA (2018) Combining temporal 3D remote sensing data with spatial rockfall simulations for improved understanding of hazardous slopes within rail corridors. *Nat Hazards Earth Syst Sci* 18(8): 2295-2308.
<https://doi.org/10.5194/nhess-18-2295-2018>
- Meng QX, Wang HL, Xu WY, et al. (2019) Numerical homogenization study on the effects of columnar jointed structure on the mechanical properties of rock mass. *Int J Rock Mech Min Sci* 124: 104127.
<https://doi.org/10.1016/j.ijrmms.2019.104127>
- Meng QX, Wang H, Cai M, et al. (2020) Three-dimensional mesoscale computational modeling of soil-rock mixtures with concave particles. *Eng Geol* 277: 105802.
<https://doi.org/10.1016/j.enggeo.2020.105802>
- Pichler B, Hellmich C, Mang HA (2005) Impact of rocks onto gravel design and evaluation of experiments. *Int J Impact Eng* 31: 560-578.
<https://doi.org/10.1016/j.ijimpeng.2004.01.007>
- Pichler B, Hellmich C, Mang HA (2006) Loading of a gravelburied steel pipe subjected to rockfall. *J Geotech Geoenviron Eng* 132: 1465-1473.
[https://doi.org/10.1061/\(ASCE\)1090-0241\(2006\)132:11\(1465\)](https://doi.org/10.1061/(ASCE)1090-0241(2006)132:11(1465))
- Tao ZG, Zhu C, He MC, et al. (2021) A physical modeling-based study on the control mechanisms of Negative Poisson's ratio anchor cable on the stratified toppling deformation of anti-inclined slopes. *Int J Rock Mech Min Sci* 138: 104632.
<https://doi.org/10.1016/j.ijrmms.2021.104632>
- Volkwein A, Kummer P, Bitnel H, et al. (2016) Load measurement on foundations of rockfall protection systems. *Sensors* 16(2): 174.
<https://doi.org/10.3390/s16020174>
- Wang XL, Frattini P, Crosta GB (2014) Uncertainty assessment in quantitative rockfall risk assessment. *Landslides* 11(4): 711-722.
<https://doi.org/10.1007/s10346-013-0447-8>
- Wang Y, Zhang B, Gao SH, et al. (2021a) Investigation on the effect of freeze-thaw on fracture mode classification in marble subjected to multi-level cyclic loads. *Theor Appl Fract Mech* 111: 102847.
<https://doi.org/10.1016/j.tafmec.2020.102847>
- Wang Y, Feng WK, Hu RL, et al. (2021b) Fracture evolution and energy characteristics during marble failure under triaxial fatigue cyclic and confining pressure unloading (FC-CPU) conditions. *Rock Mech Rock Eng* 54: 799-818.
<https://doi.org/10.1007/s00603-020-02299-6>
- Yuan JK, Li YR, Huang RQ, et al. (2015) Impact of rockfalls on protection measures: an experimental approach. *Nat Hazards Earth Syst Sci* 15(4): 885-893.
<https://doi.org/10.5194/nhess-15-885-2015>
- Zhang G, Tang, H, Xiang B (2015) Theoretical study of rockfall impacts based on logistic curves. *Int J Rock Mech Min Sci* 78: 133-143.
<https://doi.org/10.1016/j.ijrmms.2015.06.001>
- Zhu C, He MC, Karakus M, et al. (2021a) Numerical simulations of the failure process of anaclinal slope physical model and control mechanism of negative Poisson's ratio cable. *Bull Eng Geol Environ* 80: 3365-3380.
<https://doi.org/10.1007/s10064-021-02148-y>
- Zhu C, He MC, Yin Q, et al. (2021b) Numerical simulation of rockfalls colliding with a gravel cushion with varying thicknesses and particle sizes. *Geomech Geophys Geo-Energy Geo-Resour* 7: 11.
<https://doi.org/10.1007/s40948-020-00203-8>
- Zhu C, Wang DS, Xia X, et al. (2018) The effects of gravel cushion particle size and thickness on the coefficient of restitution in rockfall impacts. *Nat Hazards Earth Syst Sci* 18(6): 1811-1823.
<https://doi.org/10.5194/nhess-18-1811-2018>
- Zhu C, Tao Z, Yang S, et al. (2019) V shaped gully method for controlling rockfall on high-steep slopes in China. *Bull Eng Geol Environ* 78(4): 2731-2747.
<https://doi.org/10.1007/s10064-018-1269-7>